Accelerated Publications

Presence of Ferric Hydroxide Clusters in Mutants of *Haemophilus influenzae* Ferric Ion-Binding Protein A[†,‡]

Stephen R. Shouldice,[§] Robert J. Skene,[∥] Douglas R. Dougan,[∥] Duncan E. McRee,[∥] Leslie W. Tari,[∥] and Anthony B. Schryvers*[,§]

Department of Microbiology and Infectious Diseases, University of Calgary, Calgary, Alberta, Canada T2N 4N1, and Syrrx Inc., San Diego, California 92121

Received August 5, 2003; Revised Manuscript Received September 2, 2003

ABSTRACT: The periplasmic iron binding protein plays an essential role in the iron uptake pathway of Gram-negative pathogenic bacteria from the Pasteurellaceae and Neisseriaceae families and is critical for survival of these pathogens within the host. In this study, we report the crystal structures of two mutant forms of ferric ion-binding protein A (FbpA) from *Haemophilus influenzae* with bound multinuclear oxo−metal clusters. Crystals of site-directed mutants in the metal or anion binding ligands contain protein in the open conformation, and two mutant FbpAs, H9A and N175L, contain different cluster arrangements in the iron-binding pocket. The iron clusters are anchored by binding to the two tyrosine ligands (Tyr195 and Tyr196) positioned at the vertex of the iron-binding pocket but are not coordinated by the other metal binding ligands. Our results suggest that the metal clusters may have formed *in situ*, suggesting that the mutant FbpAs may serve as a simple model for protein-mediated mineralization.

Because of the importance of iron in biological processes, various organisms have developed specialized mechanisms for acquiring, transporting, and storing this essential element (*1*). In humans and other vertebrates, iron is obtained from dietary intake through absorption by mucosal cells in the jejunum (*2*). Within the body, iron is transported from areas of supply to areas of need by the serum glycoprotein transferrin (Tf).[1] Because of its high affinity for iron, transferrin effectively sequesters free iron released into the extracellular environment. On mucosal surfaces and at sites of infection, the related glycoprotein, lactoferrin, fulfills this role. Collectively, these monomeric, bilobed glycoproteins are responsible for reducing the concentration of free ferric iron in the extracellular milieu to a level below which microbial growth can occur (*3*). Pathogenic bacterial species require high-affinity iron uptake systems capable of acquiring iron from these host proteins to grow and survive within the host (*4*).

Pathogenic Gram-negative bacteria in the Neisseriaceae and Pasteurellaceae families possess high-affinity iron acquisition mechanisms that involve direct binding of the host glycoproteins by specific receptors at the cell surface (*5*). The surface receptor, which is comprised of two proteins, Tf binding protein A (TbpA) and Tf binding protein B (TbpB), mediates iron removal and transport across the outer membrane. TbpA is a TonB-dependent outer membrane protein that is proposed to function as an integral membrane-gated porin through which iron removed from Tf is translocated. The ability of TbpA to function in this capacity requires a functional TonB and associated proteins (ExbB and ExbD) (*6*). The TbpB component of the receptor is an extrinsic lipoprotein, which is thought to play a facilitory role in the initial stages of the iron acquisition process (*7*). The subsequent transport of iron from the periplasmic space into the bacterial cell interior is mediated by a periplasmic ferric binding protein and an inner-membrane permease complex composed of transmembrane and ATPase components (*8*).

Within the cell, ferrous iron is either incorporated into various biosynthetic enzymes or electron transport proteins or converted into a multinuclear storage form by one of the available ferritins. The non-heme ferritin encoded by the *ftn* gene has been shown to be involved in iron storage, whereas the role of bacterioferritin, encoded by the *bfr* gene, remains unclear (*9*). Ferritin forms a tetracosameric structure composed of 24 subunits which catalyzes the formation of oxo-

[†] This work was supported by Grant 49603 from the Canadian Institutes of Health Research.

[‡] The PDB entries for the H9A and N175L mutant FbpAs are 1QVS and 1QW0, respectively.

* To whom correspondence should be addressed: Department of Microbiology and Infectious Diseases, University of Calgary, Rm. 274, Heritage Medical Research Building, 3330 Hospital Dr., N.W., Calgary, Alberta, Canada T2N 4N1. Telephone: (403) 220-3703. Fax: (403) 270-2772. E-mail: schryver@ucalgary.ca.

[§] University of Calgary.

[∥] Syrrx Inc.

[1] Abbreviations: FbpA, ferric binding protein A; Tf, transferrin; TbpA, transferrin binding protein A; TbpB, transferrin binding protein B; IPTG, isopropyl thiogalactoside; HPLC, high-pressure liquid chromatography; EDTA, ethylenediaminetetraacetic acid; PEG, polyethylene glycol; MME, monomethyl ether.

10.1021/bi035389s CCC: $25.00
Published on Web 09/26/2003

bridged Fe(III) dimers and can ultimately accumulate complexes with up to 2000 iron atoms per tetracosameric shell (*10*).

Although the host glycoproteins and the bacterial periplasmic binding proteins operate in different compartments, they have striking similarities in their overall structure and mechanism of iron binding, as both belong to the transferrin structural superfamily (*11*, *12*). Transferrins are composed of two structurally equivalent lobes, each of which contains an iron binding site located in a cleft between two globular domains connected by two antiparallel β-strands (*13*). FbpA resembles a single lobe of transferrin, consisting of two domains connected by antiparallel β-strands (*12*, *14*). Other similarities between the two molecules include an alternating helix−sheet folding motif and coordination of iron by six ligands in nearly perfect octahedral geometry, with four similar amino acids that directly coordinate with the ferric ion. In transferrins and in FbpA, the liganding amino acids are present on both domains and there is a substantial movement of the individual domains relative to one another upon iron release (*14*−*16*).

Despite the overall similarities, there are some notable differences between transferrins and FbpA. First, transferrin utilizes an exogenous carbonate as the coordinating anion, whereas the FbpA utilizes a phosphate anion (*12*). Second, the transferrin iron-binding site is substantially less solvent-exposed than that of FbpA. This is due in part to the different location of the liganding amino acids on the polypeptide chain.

The iron binding properties of transferrins have been extensively studied, resulting in several proposed mechanisms of iron binding and release (*17*). Analyses of site-directed mutants of transferrin (*18*, *19*) and its N-lobe (*20*−*23*) have provided insights into the mechanism of iron release and have confirmed the role of the liganding amino acids in metal ion binding. We sought to explore the role of similar mutations in FbpA. In this study, we report on the preparation and analysis of two site-directed mutants of the FbpA from *Haemophilus influenzae* which were carried out to explore the similarities and differences between FbpAs and transferrins. Since the FbpABC pathway has been proposed as a target for the development of broad-spectrum antimicrobial agents (*12*), it will be important to fully appreciate the similarities and differences between the bacterial and host proteins.

MATERIALS AND METHODS

Purification of FbpA. Mutant *H. influenzae* FbpAs (H9A and N175L) were expressed from a recombinant pT7-7 plasmid after induction with IPTG in the BL21(DE3)pLysS host strain. A modified osmotic shock procedure provided relatively pure preparations of the protein (*24*). Samples were then extensively dialyzed against 10 mM Tris buffer (pH 7.5) at 4 °C and subjected to cation exchange chromatography on a BioCad HPLC system (PerSeptive Biosystems) as a final purification step. The column was washed with 10 volumes of 20 mM Tris buffer (pH 7.5) to remove unbound proteins and eluted with a gradient of 0 to 1.5 M NaCl. Once purified protein was obtained, it was concentrated using a Centricon 10 microconcentrator. Following concentration, the sample still in the Centricon was exhaustively exchanged into 10 mM Tris buffer (pH 8.0) to remove excess salt. After concentration, the removal of metal ions from the proteins for spectral analysis was accomplished by the addition of 1 mM EDTA and a 4000-fold molar excess of sodium citrate (pH 7.0) followed by incubation of the samples on ice for 20 min. The protein solutions were again exchanged into 10 mM Tris buffer (pH 8.0). To provide phosphate as a synergistic anion, 5 mM phosphate was added to the sample which was incubated on ice for an additional 20 min. After the samples had been washed with buffer, a solution of freshly prepared 16 mg/mL ferric chloride in 100 mM sodium citrate and 100 mM sodium carbonate (pH 8.0) was added to the samples to provide a 5-fold molar excess of iron and left overnight at 4 °C. After being washed with buffer, the samples were dialyzed extensively against 10 mM Tris buffer (pH 8.0) at 4 °C. The resulting preparations were deemed pure on the basis of SDS−PAGE analysis (data not shown). Both proteins were stored at −80 °C until they were used for crystallography.

Crystallization and Data Collection. Iron-loaded protein samples were removed from a −80 °C environment and placed on ice to thaw. The crystals of the mutant FbpA proteins were grown by vapor diffusion using the hanging drop technique. The mutant proteins were initially screened around the conditions already determined for the iron-loaded wild-type protein (*12*). Since these conditions had proven to be successful for the metal-loaded wild-type protein, they served as a starting point in attempts to crystallize the mutated FbpAs. Following the initial crystallization experiments, further conditions were then screened to optimize the crystallization conditions. Crystals of H9A were grown at 4 °C by the hanging drop technique from 4 μL drops containing 15 mg/mL of the H9A FbpA, 18% polyethylene glycol (PEG) 550 monomethyl ether (MME), and 0.05 M Tris (pH 7.6). The drops were equilibrated against a 1 mL reservoir containing 36% PEG 550 MME and 0.1 M Tris (pH 7.6). Similarly, crystals of N175L FbpA were grown using hanging drops at 4 °C in 4 μL drops containing 20 mg/mL N175L FbpA, 18% PEG 550 MME, and 0.05 M Tris (pH 8.2). These drops were equilibrated against a 1 mL reservoir containing 36% PEG 550 MME and 0.1 M Tris (pH 8.2). Diffraction quality crystals typically grew after 4 days. For cryocrystallography, crystals were placed in a cryoprotectant solution identical to the reservoir solution with a final ethylene glycol concentration of 20% (v/v) for a short time before being placed in the nitrogen gas stream to be cooled to 100 K.

Initial X-ray analysis revealed that all crystals belong to the orthorhombic space group $P2_12_12$ with the cell parameters outlined in Table 1 and with one subunit in the asymmetric unit. All X-ray data sets were collected from single crystals at 100 K using cryomounting procedures. Data from H9A were recorded on a Bruker CCD detector using a Rigaku FR-D rotating anode with a Cu target and were processed using Proteum software. Data from the N175L crystal were also recorded on a Rigaku R-Axis HTC three-image plate detector system with a Rigaku FR-D rotating anode generator producing Cu Kα X-rays. A Rigaku X-stream 2000 cryosystem was used to keep the crystals at a temperature of 100 K. All data sets were merged and scaled using either the Proteum or CrystalClear suite of programs. The data sets were collected at a wavelength of 1.5418 Å and were more

Table 1: Summary of Crystallographic Data

	H9A	N175L
data collection		
wavelength (Å)	1.5418	1.5418
resolution (Å)	62−2.1	62−1.9
unit cell dimensions (Å)	$a = 106.00$, $b = 75.66$, $c = 33.77$	$a = 105.85$, $b = 76.04$, $c = 34.07$
completeness (%)[a]	97.4 (92.7)	97.2 (90.8)
$I/\sigma(I)$	14.1 (5.3)	18.6 (3.5)
R_{sym}[b]	0.075 (0.187)	0.063 (0.168)
redundancy	3.3	5.7
refinement statistics		
resolution (Å)	62−2.1	62−1.9
completeness for range (%)	97.0	97.3
no. of reflections[c]	15136	20739
working set	14326	19620
free set	810	1119
R-factor[d]	0.168	0.220
R_{free}	0.226	0.271
no. of protein atoms	4522	4504
no. of waters	300	196
no. of Fe atoms	3	4
no. of PO_4 molecules	2	1
mean B-factor (Å^2)	12.99	19.03
rms deviation from ideality		
bond lengths (Å)	0.009	0.009
bond angles (deg)	1.074	1.087

[a] The number in parentheses is the statistic for the highest-resolution shell. [b] $R_{sym} = \sum_h(\sum_j|I_{j,h} - \langle I_h\rangle|/\sum I_{j,h})$, where h represents a set of Miller indices and j represents a set of observations of reflection h. [c] $F > 2.0\sigma$. [d] R-factor $= \sum_{hkl}|F_o - F_c|/\sum_{hkl}|F_o|$.

than 97% complete. Individual data processing statistics for the mutants are listed in Table 1.

Structure Solution and Refinement. To determine the structure of the mutant FbpAs by molecular replacement, the structure of apo *H. influenzae* was used as the initial phasing model. The atomic coordinates of the 1.75 Å model of the apo form of *H. influenzae* FbpA (1D9V) were obtained from the Protein Data Bank (*14*). The phosphate anion and all the water molecules were removed from the initial model. First, rigid body refinement was carried out to allow for the slight cell dimension changes with the FbpA apo form refined as a whole body. A $2|F_o| - |F_c|\alpha_c$ electron density map was calculated revealing interpretable electron density depicting the unit cell contents of each FbpA. Each model was refined using Refmac5 with maximum likelihood refinement against structure factors (*25*). Five percent of the reflections were set aside for calculation of R_{free}, and the same set of test reflections was maintained throughout the refinement process. Iterative cycles of manual refitting of each model and refinement were carried out to complete and correct each model. Water molecules were then incorporated into each model using the program ARP/wARP. A final inspection of density using $2|F_o| - |F_c|\alpha_c$ and $|F_o| - |F_c|\alpha_c$ maps was used to explain any remaining unassigned density. Electron densities of several surface-exposed side chains were missing in each protein and modeled as alanines. Individual refinement statistics for the metal-binding mutants are displayed in Table 1.

RESULTS

Overall Structure. Each of the iron-loaded mutant FbpA proteins crystallized in the orthorhombic space group $P2_12_12$

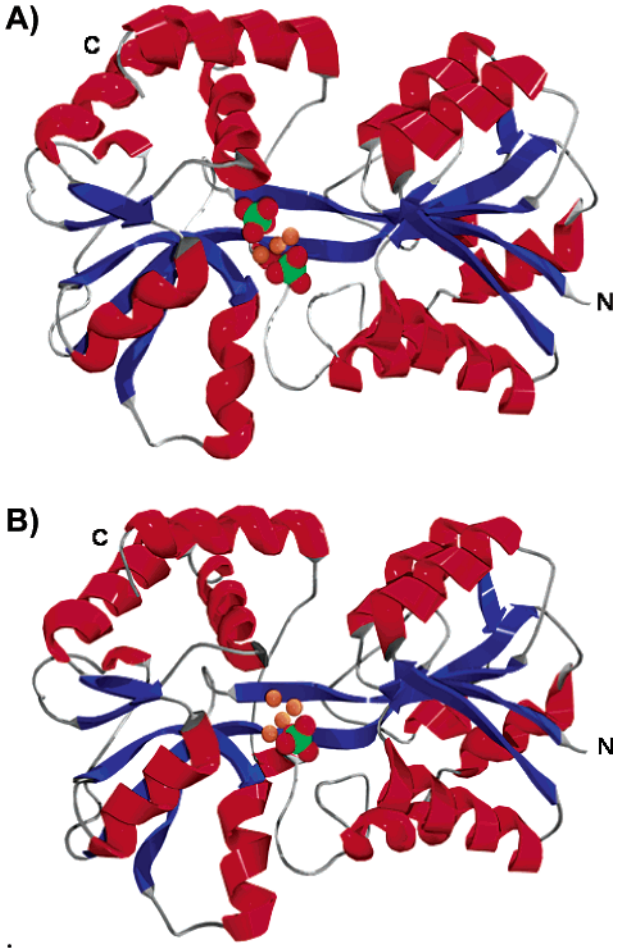

FIGURE 1: Ribbon diagrams of (A) H9A and (B) N175L FbpA. FbpA possesses two α/β domains linked by a pair of β-strands. α-Helices are shown in red, while β-strands are shown in blue. The relative binding modes of the iron atoms (orange) and phosphate anion(s) found in the structures are shown.

with one complex in each asymmetric unit, with unit cell dimensions similar to those of the H9Q mutant and the apo wild-type structure (*14*, *24*). Data collection and refinement statistics are reported for each protein in Table 1. The final C-terminal amino acid (residue 309 along with residue 308 in N175L) could not be modeled for either protein and is deleted from the final structures. The electron density surrounding the remainder of each protein is continuous, allowing for the unambiguous tracing of the polypeptide chain. Electron density for several side chains of surface-exposed residues was also missing, and the affected side chains were built as alanines in the final models.

The overall structure of each of the mutant FbpAs is very similar to the apo wild-type structure (*14*). The quality of each protein structure is excellent, with more than 90% of the amino acid residues occupying the most favorable regions of a Ramachandran plot (data not shown). Figure 1 shows that each of these proteins possesses the same polypeptide topology as the wild-type protein, consisting of two globular domains, each centered on a mixed β-sheet surrounded by α-helices. A hinge region consisting of a pair of antiparallel β-strands connects these globular domains. As in the wild-type apo structure, there is a hinge movement of the two globular domains with hinge angle that is ~20° greater than that in the holo form. An overlay of the C_α backbone of FbpA from the apo form with the H9A and N175L proteins

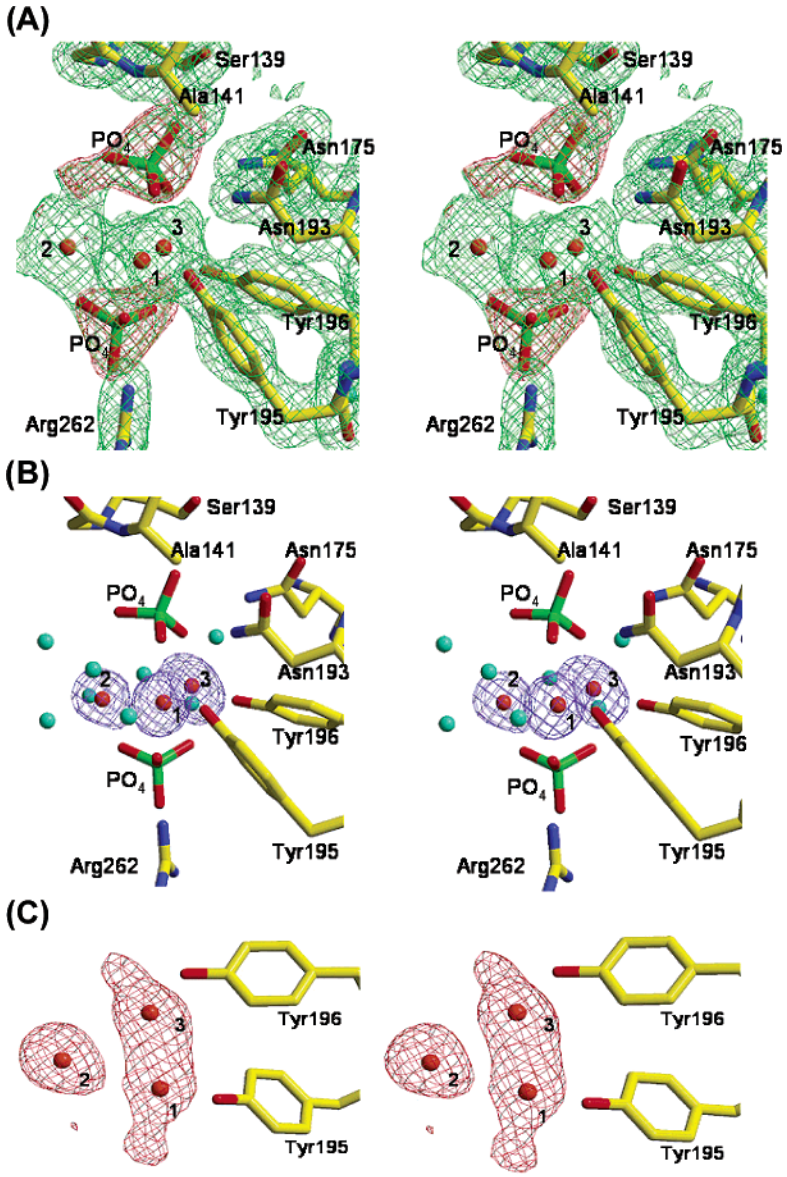

FIGURE 2: Stereoviews showing the iron-binding site of H9A FbpA. (A) Electron density maps (green for the $2F_o - F_c$ map contoured at 1σ and orange for the $F_o - F_c$ map contoured at 3σ) obtained using the reflection data of the H9A protein after refinement of the model in which the phosphate molecules were omitted. (B) Anomalous difference Fourier density map contoured at 3σ (purple) calculated with exclusion of the iron atoms. (C) Electron density map ($2F_o - F_c$, red) contoured at 5σ obtained using the reflection data of the H9A protein after refinement of the model from which the iron atoms were omitted. This view is rotated 90° relative to panels A and B. The final model is superimposed in stick presentation with atoms in standard colors. This figure was generated by Raster 3D (*40*).

gives root-mean-square deviations of 0.34 and 0.27 Å, respectively.

In the holo wild-type structure, six ligands octahedrally coordinate a single ferric ion between the two globular domains (*12*). The protein itself contributes two ligands, His9 and Glu57, from the N-terminal domain and two ligands, Tyr195 and Tyr196, from the C-terminal domain (*12*). The final two ligands are provided by a water molecule and an exogenous phosphate ion (*26*). Two different Fe^{3+} ion clusters were present in the metal-binding pockets of the mutant proteins. A trinuclear cluster was observed for the H9A mutant, while a tetranuclear cluster was seen in the case of the N175L mutation (Figures 2 and 3). Despite the differences in the observed clusters, the ferric ions in either mutant structure are not in direct contact with any of the protein atoms, except for the tyrosinate oxygen ligands of Tyr195 and Tyr196. Thus, the side chains of Glu57 and His9 (N175L mutant) are swung away from the iron-binding site.

H9A Trinuclear Cluster. The N-terminal domain does not appear to be in direct contact with any of the iron atoms of the cluster, suggesting that this domain may be mobile in solution. Negatively charged hydroxide and phosphate oxygen atoms are utilized to coordinate Fe^{3+} ions and connect them in a manner similar to the structure of the mineral Fe_2O_3 (*27*), with each ferric ion coordinated in a distorted octahedral arrangement. Trinuclear cores containing ferrous or ferric forms of iron ions are common in inorganic complexes possessing various chemical forms of oxygen ligands (*28*−*30*). The trinuclear cluster present in the H9A protein possesses a construction similar to that of a ferric end member of the oxidized mineral vivianite (*28*). All three ferric ions are well-ordered in the H9A structure with

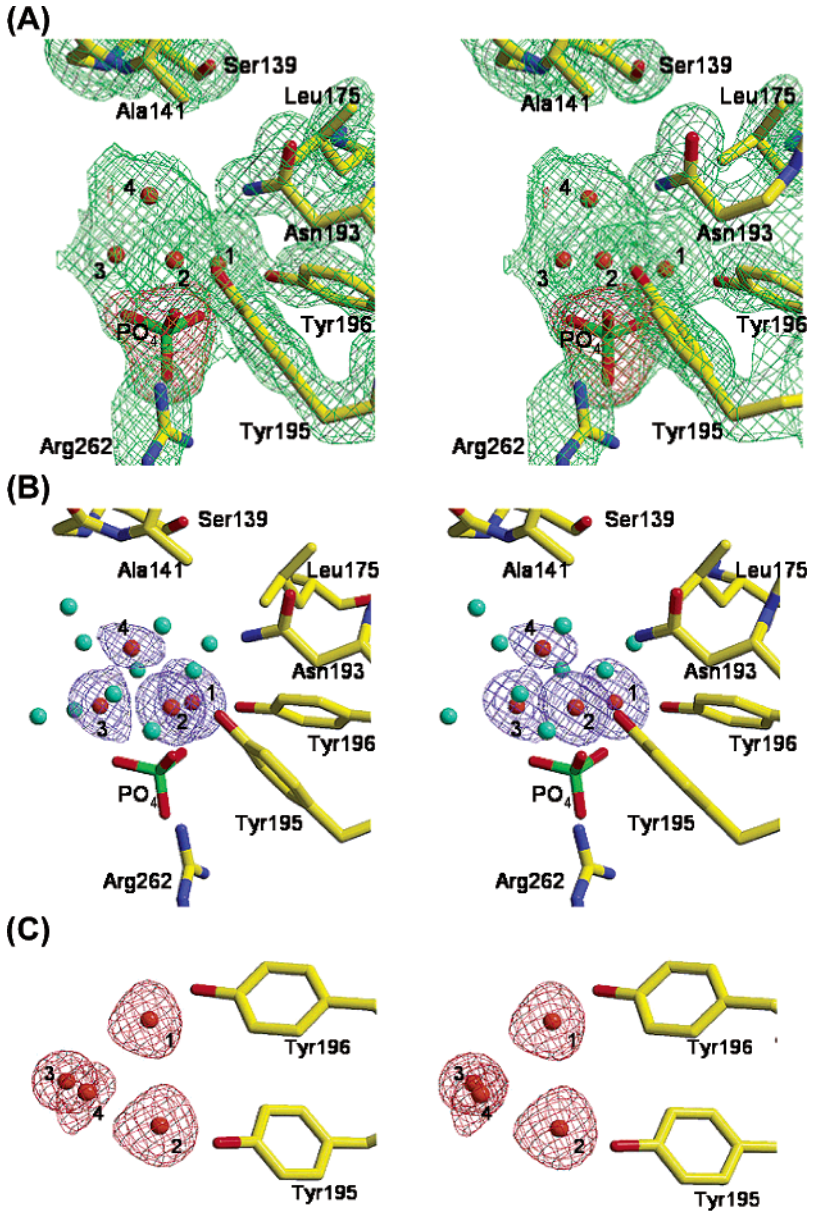

FIGURE 3: Stereoviews depicting the iron-binding site of N175L FbpA. (A) Electron density maps (green for the $2F_o - F_c$ map contoured at 1σ and orange for the $F_o - F_c$ map contoured at 3σ) obtained using the reflection data of the N175L protein after refinement of the model from which the phosphate molecule was omitted. (B) Anomalous difference Fourier density map contoured at 3σ (purple) calculated with exclusion of the iron atoms. (C) Electron density map ($2F_o - F_c$, red) contoured at 5σ obtained using the reflection data of the N175L protein after refinement of the model from which the iron atoms were omitted. This view is rotated 90° relative to panels A and B. The final model is superimposed in stick presentation with atoms in standard colors. This figure was generated by Raster 3D (*40*).

individual *B*-factors ranging from 30 to 40 Å^2, with Fe−Fe distances ranging from 2.8 to 3.4 Å which is within the range of other well-refined iron-containing structures (*10*, *31*) (Figure 2).

This cluster has two phosphate anions associated with it. One phosphate molecule is located in the previously determined ternary anion-binding site (*12*, *14*). The other phosphate is positioned on the opposite side of the cluster and forms hydrogen bonds (3.0 and 3.2 Å) with arginine 262 much like the carboxylate group of EDTA in the H9Q structure (*24*). Each metal ion is coordinated by six oxygen atoms in a distorted octahedral arrangement with Fe−O distances ranging from 1.9 to 3.0 Å. The Fe−tyrosinate bonds are the shortest of the cluster. Although Tyr195 O and Tyr196 O are the only amino acid atoms that interact directly with the ferric iron, they too have changed and are now located 4.7 Å away from each other, which is significant when compared to a distance of 3.0 Å in the wild-type holo FbpA structure, where both tyrosines bind a single Fe^{3+} (*12*).

N175L Tetranuclear Cluster. This protein also crystallized in an open conformation when compared to the apo and holo wild-type structures. The mutation in N175L results in the loss of one of the ligands involved in anion binding at the ternary anion-binding site (*14*). With the absence of the phosphate anion, a fourth ferric ion is present in this cluster compared to the previous trinuclear cluster. As in the previous cluster, the Fe1−Fe3 ions are fully ordered (Figure 3). The additional Fe^{3+} points slightly toward the vacant anion-binding site and also into the solvent. A high electron density peak (5σ) and strong anomalous difference density peak (3σ) confirm that it is an iron; however, the high temperature factor associated with this atom (60 Å^2) indicates

that it is mobile or a partially occupied site. The Fe−Fe distances range from 2.6 to 3.6 Å, falling in the range of other published structures (*10*, *31*).

As in the trinuclear cluster, the oxygen atoms coordinating each iron atom are distorted from octahedral symmetry, with Fe−O distances ranging from 1.8 to 2.9 Å. Like in the trinuclear cluster, the phosphate molecule located on the opposite side of the cluster forms hydrogen bonds with arginine 262 (3.1 and 3.2 Å). The O groups of residues 195 and 196 have moved even further apart in the tetranuclear cluster (5.3 Å) than in the previous structure as once again each group is utilized to coordinate a separate Fe^{3+} unlike the wild-type structure.

DISCUSSION

Members of the transferrin structural superfamily, transferrin, lactoferrin, and FbpA, use a similar octahedral coordination complex to achieve high-affinity binding of ferric ion. There are two tyrosinate oxygen ligands, an imidazole nitrogen from a histidine and a carboxylate oxygen from an acidic residue (Asp in Tf and Lf and Glu in FbpA). The coordination is completed by two carbonate anion oxygens in Tf and Lf and by a phosphate oxygen and a water oxygen in FbpA (*12*). The amino acids responsible for binding to the iron atom or the participating anion reside in different regions of the protein in such a manner that metal binding is accompanied by substantial movement of the two domains, aptly described as a change from the open to closed conformation (*14*, *16*, *32*). The metal-bound forms of Tf, Lf, and FbpA have been crystallized in the closed conformation, suggesting that this may be the favored conformation in solution. In contrast, the open conformation is thought to be the favored conformation of the apo form in solution, since this is the conformation preferentially found in crystal structures of apo forms of the proteins (*14*−*16*, *33*).

As a complement to biochemical and functional studies, we determined the structures of metal-bound forms of eight different site-directed mutants of the *H. influenzae* FbpA: H9A, H9Q, E57A, Q58L, Y195A, Y196A, N175L, and N193L. A surprising finding was that all of these proteins crystallized in the open conformation (Figure 1, ref *24*, and data not shown), in contrast to the closed conformation of the metal-bound wild-type protein (*12*). This may suggest that the open conformation is a common, if not preferred, conformation of the site-directed FbpA mutant proteins and implies that the liganding residues may play an essential role in domain closure. In contrast to what is observed for the FbpA proteins, metal-bound forms of site-directed mutants of Tf and Lf crystallized in the closed conformation (*23*, *34*−*37*). The binding cleft is substantially deeper in these proteins, and additional interactions between residues from the two domains likely contribute to stabilizing the closed conformation.

The observation that two of the mutant *H. influenzae* FbpA proteins contain ferric hydroxide clusters (Figures 2 and 3) clearly demonstrates that these proteins are capable of binding to iron complexes of this size, which is similar to the demonstration of Hf^{4+} clusters in the *Neisseria gonorrheae* FbpA (*38*). In this previous study, the wild-type apoprotein was exposed to excesses (up to 100-fold) of the metal (Fe^{3+}, Ti^{4+}, Zr^{4+}, or Hf^{4+}) and yielded metal:protein ratios as high as 4:1. Since exposure of the native holoprotein to excess metal did not alter the 1:1 metal:protein ratio, the authors concluded that FbpA was binding existing metal complexes present in the solution (*38*). The conformational heterogeneity in the Hf^{4+}-containing crystals, with variations in the interdomain hinge angle and in the size of the metal clusters, is consistent with this proposal.

In contrast to the previous study, our results do not suggest binding of pre-existing metal complexes, and in the absence of direct experimental evidence to the contrary, we should also consider the formation of the complexes *de novo*. It is important to note that the apo forms of the eight different FbpA mutants were exposed to merely a 5-fold molar excess of iron and that only two of the mutant protein structures had more than one iron atom bound. If the tetranuclear cluster in the N175L mutant protein (Figure 3) was due to binding of preformed clusters, it would infer that nearly 80% of the iron in the citrate/carbonate solution was in that form. Similarly, a majority of the iron in the buffer would have to be in a trinuclear form to account for its presence in the H9A FbpA structure. Thus, we propose that since these mutant proteins may remain predominantly in the open conformation, the ferric hydroxide complex may form *in situ* in a process that in some ways may be analogous to the formation of ferric ion clusters in ferritin. This proposal could be addressed by exposing crystals with a single ferric ion present to exogenous iron and determine whether ferric hydroxide clusters can be formed. The crystals of the other mutant FbpAs or new crystals prepared from the H9A and N175L FbpAs loaded with lower levels of ferric ions would be obvious candidates for these experiments.

The mutant FbpAs may provide a simple model for protein-mediated mineralization with the advantage of providing structural information about the metal clusters that are formed. The protein-mediated mineralization by ferritins is a much more complex and extensively studied process in which interestingly, tyrosyl residues have been shown to play a key role in mineralization (*39*). Although bound metal ions are observed in structures of ferritins (*10*), they do not include the higher-order metal clusters observed in the FbpA structures. Thus, it is possible that studies with mutant FbpAs might provide interesting insights that would be difficult to acquire from studies with ferritins.

The role of ligands in metal binding by transferrin and lactoferrin has been evaluated by numerous studies using site-directed mutations of the recombinant proteins, particularly with the N-lobe. Replacement of histidine 249 of the N-lobe of human transferrin with alanine, glutamic acid, or glutamine resulted in a significant alteration in binding properties, with increases in the rate constants for iron removal ranging from 3- to 150-fold (*22*). Structural studies with the H249E mutant demonstrated that the glutamic acid residue effectively replaced histidine in coordination of iron, accounting for the relatively stable metal binding by this mutant protein (*23*). In the H249Q mutant protein, the glutamine also participated in coordination of iron, but with a longer Fe−Oϵ1 bond (*34*), which correlates with the increased rate constant for iron removal. Although no structure for H249A is currently available, it is believed that a water molecule or some other anion would be used to coordinate in the absence of an appropriate side chain. Site-directed mutant studies with the equivalent ligand of the *H.*

influenzae FbpA, histidine 9, yielded structures of the protein in the open conformation with either a metal chelate (*24*) or a multinuclear cluster (Figure 2). Although preliminary iron removal studies with the H9A protein suggested only a moderate alteration in release kinetics (data not shown), the potential presence of iron clusters in the protein clearly jeopardizes interpretation of the results. In view of the proposed propensity of mutant FbpAs to remain in the open conformation and the potential for accommodating various iron complexes, it will be essential to ensure that monoferric forms of the protein are prepared and maintained for evaluation of iron binding properties.

The production and characterization of site-directed mutants of transferrin and lactoferrin, particularly in the recombinant N-lobes of these proteins, have provided substantial insights into their metal binding properties, particularly when coupled to structural studies of these proteins. This approach can clearly provide similar insights into the metal binding properties of the bacterial periplasmic iron-binding proteins, provided that the methods for assessment of iron binding capabilities take into account the potential for these proteins to accommodate various metal complexes. The bacterial proteins afford an additional advantage by providing the opportunity to evaluate the functional properties of the mutant proteins *in vivo*, which can be readily accomplished by facile gene replacement approaches. Comparable experiments with transferrins and lactoferrins would clearly be more elusive.

ACKNOWLEDGMENT

We are indebted to Syrrx Inc. for allowing us to use laboratory space and beam time for the completion of this project.

REFERENCES

1. Weinberg, E. D., and Weinberg, G. A. (1995) *Curr. Opin. Infect. Dis. 8*, 164−169.
2. Ratledge, C., and Dover, L. G. (2000) *Annu. Rev. Microbiol. 54*, 881−941.
3. Braun, V., and Killmann, H. (1999) *Trends Biochem. Sci. 24*, 104−109.
4. Mietzner, T. A., Tencza, S. B., Adhikari, P., Vaughan, K. G., and Nowalk, A. J. (1998) *Curr. Top. Microbiol. Immunol. 225*, 113−135.
5. Gray-Owen, S. D., and Schryvers, A. B. (1996) *Trends Microbiol. 4*, 185−191.
6. Schryvers, A. B., and Stojiljkovic, I. (1999) *Mol. Microbiol. 32*, 1117−1123.
7. Anderson, J. A., Sparling, P. F., and Cornelissen, C. N. (1994) *J. Bacteriol. 176*, 3162−3170.
8. Adhikari, P., Berish, S. A., Nowalk, A. J., Veraldi, K. L., Morse, S. A., and Mietzner, T. A. (1996) *J. Bacteriol. 178*, 2145−2149.
9. Abdul-Tehrani, H., Hudson, A., Chang, Y.-S., Timms, A., Hawkins, C., Williams, J., Harrison, P., Guest, J., and Andrews, S. (1999) *J. Bacteriol. 181*, 1415−1428.
10. Stillman, T. J., Hempstead, P. D., Artymiuk, P. J., Andrews, S. C., Hudson, A. J., Treffry, A., Guest, J. R., and Harrison, P. M. (2001) *J. Mol. Biol. 307*, 587−603.
11. Nowalk, A. J., Tencza, S. B., and Mietzner, T. A. (1994) *Biochemistry 33*, 12769−12775.
12. Bruns, C. M., Norwalk, A. J., Avrai, A. S., McTigue, M. A., Vaughan, K. A., Mietzner, T. A., and McRee, D. E. (1997) *Nat. Struct. Biol. 4*, 919−924.
13. Baker, E. N., and Lindley, P. F. (1992) *J. Inorg. Biochem. 47*, 147−160.
14. Bruns, C. M., Anderson, D. S., Vaughan, K. G., Williams, P. A., Nowalk, A. J., McRee, D. E., and Mietzner, T. A. (2001) *Biochemistry 40*, 15631−15637.
15. Jeffrey, P. D., Bewley, M. C., MacGillivray, R. T. A., Mason, A. B., Woodworth, R. C., and Baker, E. N. (1998) *Biochemistry 37*, 13978−13986.
16. Anderson, B. F., Baker, H. M., Norris, G. E., Rumball, S. V., and Baker, E. N. (1990) *Nature 344*, 784−787.
17. Kuser, P., Hall, D. R., Haw, M. L., Neu, M., Evans, R. W., and Lindley, P. F. (2002) *Acta Crystallogr. D58*, 777−783.
18. Zak, O., Tam, B., MacGillivray, R. T. A., and Aisen, P. (1997) *Biochemistry 36*, 11036−11043.
19. Mason, A. B., He, Q. Y., Tam, B. M., MacGillivray, R. T. A., and Woodworth, R. C. (1998) *Biochem. J. 330*, 35−40.
20. Woodworth, R. C., Mason, A. B., Funk, W. D., and MacGillivray, R. T. A. (1991) *Biochemistry 30*, 10824−10829.
21. He, Q. Y., Mason, A. B., Woodworth, R. C., Tam, B. M., Wadsworth, T., and MacGillivray, R. T. A. (1997) *Biochemistry 36*, 5522−5528.
22. He, Q. Y., Mason, A. B., Pakdaman, R., Chasteen, N. D., Dixon, B. K., Tam, B. M., Nguyen, V., MacGillivray, R. T. A., and Woodworth, R. C. (2000) *Biochemistry 39*, 1205−1210.
23. MacGillivray, R. T. A., Bewley, M. C., Smith, C. A., He, Q. Y., Mason, A. B., Woodworth, R. C., and Baker, E. N. (2000) *Biochemistry 39*, 1211−1216.
24. Shouldice, S. R., Dougan, D. R., Skene, R. J., Tari, L. W., McRee, D. E., Yu, R.-H., and Schryvers, A. B. (2003) *J. Biol. Chem. 278*, 11513−11519.
25. Collaborative Computational Project No. 4 (1994) *Acta Crystallogr. D50*, 760−763.
26. Taboy, C. H., Vaughan, K. G., Mietzner, T. A., Aisen, P., and Crumbliss, A. L. (2001) *J. Biol. Chem. 276*, 2719−2724.
27. Blake, R. L., Hessevick, R. E., Zoltai, T., and Finger, L. W. (1966) *Am. Mineral. 51*, 123−129.
28. Moore, P. B. (1970) *Am. Mineral. 56*, 1−17.
29. Moore, P. B., and Araki, T. (1975) *Am. Mineral. 60*, 454−459.
30. Janney, D. E., Cowley, J. M., and Buseck, P. R. (2000) *Am. Mineral. 85*, 1180−1187.
31. Stout, C. D. (1989) *J. Mol. Biol. 205*, 545−555.
32. Gerstein, M., Anderson, B. F., Norris, G. E., Baker, E. N., Lesk, A. M., and Chothia, C. (1993) *J. Mol. Biol. 234*, 357−372.
33. Kurokawa, H., Dewan, J. C., Mikami, B., Sacchettini, J. C., and Hirose, M. (1999) *J. Biol. Chem. 274*, 28445−28452.
34. Baker, H. M., Mason, A. B., He, Q. Y., MacGillivray, R. T., and Baker, E. N. (2001) *Biochemistry 40*, 11670−11675.
35. Faber, H. R., Bland, T., Day, C. L., Norris, G. E., Tweedie, J. W., and Baker, E. N. (1996) *J. Mol. Biol. 256*, 352−363.
36. Faber, H. R., Baker, C. J., Day, C. L., Tweedie, J. W., and Baker, E. N. (1996) *Biochemistry 35*, 14473−14479.
37. Nicholson, H., Anderson, B. F., Bland, T., Shewry, S. C., Tweedie, J. W., and Baker, E. N. (1997) *Biochemistry 36*, 341−346.
38. Alexeev, D., Zhu, H., Guo, M., Zhong, W., Hunter, D. J., Yang, W., Campopiano, D. J., and Sadler, P. J. (2003) *Nat. Struct. Biol. 10*, 297−301.
39. Pereira, A. S., Tavares, P., Lloyd, S. G., Danger, D., Edmondson, D. E., Theil, E. C., and Huynh, B. H. (1997) *Biochemistry 36*, 7917−7927.
40. Merritt, E., and Bacon, D. (1997) *Methods Enzymol. 277*, 505−524.

BI035389S